Insights into the surface composition and enrichment effect of ionic liquids and ionic liquid mixtures

ARTICLE *in* PHYSICAL CHEMISTRY CHEMICAL PHYSICS · FEBRUARY 2010

Impact Factor: 4.49 · DOI: 10.1039/b920804f · Source: PubMed

8 AUTHORS, INCLUDING:

Till Cremer
Incom Inc.
22 PUBLICATIONS **766** CITATIONS
SEE PROFILE

Claudia Kolbeck
Friedrich-Alexander-University of Erlangen-…
21 PUBLICATIONS **694** CITATIONS
SEE PROFILE

Peter S Schulz
Friedrich-Alexander-University of Erlangen-…
56 PUBLICATIONS **1,141** CITATIONS
SEE PROFILE

This paper is published as part of a PCCP Themed Issue on:
Physical Chemistry of Ionic Liquids

Guest Editor: Frank Endres (Technical University of Clausthal, Germany)

Editorial

Perspectives

Discussion

Papers

Patterns of protein unfolding and protein aggregation in ionic liquids
Diana Constatinescu, Christian Herrmann and Hermann Weingärtner, *Phys. Chem. Chem. Phys.*, 2010, **DOI:** 10.1039/b921037g

High vacuum distillation of ionic liquids and separation of ionic liquid mixtures
Alasdair W. Taylor, Kevin R. J. Lovelock, Alexey Deyko, Peter Licence and Robert G. Jones, *Phys. Chem. Chem. Phys.*, 2010, **DOI:** 10.1039/b920931j

Designer molecular probes for phosphonium ionic liquids
Robert Byrne, Simon Coleman, Simon Gallagher and Dermot Diamond, *Phys. Chem. Chem. Phys.*, 2010, **DOI:** 10.1039/b920580b

States and migration of an excess electron in a pyridinium-based, room-temperature ionic liquid: an *ab initio* molecular dynamics simulation exploration
Zhiping Wang, Liang Zhang, Robert I. Cukier and Yuxiang Bu, *Phys. Chem. Chem. Phys.*, 2010, **DOI:** 10.1039/b921104g

J-aggregation of ionic liquid solutions of *meso*-tetrakis(4-sulfonatophenyl)porphyrin
Maroof Ali, Vinod Kumar, Sheila N. Baker, Gary A. Baker and Siddharth Pandey, *Phys. Chem. Chem. Phys.*, 2010, **DOI:** 10.1039/b920500d

Spontaneous product segregation from reactions in ionic liquids: application in Pd-catalyzed aliphatic alcohol oxidation
Charlie Van Doorslaer, Yves Schellekens, Pascal Mertens, Koen Binnemans and Dirk De Vos, *Phys. Chem. Chem. Phys.*, 2010, **DOI:** 10.1039/b920813p

Electrostatic interactions in ionic liquids: the dangers of dipole and dielectric descriptions
Mark N. Kobrak and Hualin Li, *Phys. Chem. Chem. Phys.*, 2010, **DOI:** 10.1039/b920080k

Insights into the surface composition and enrichment effects of ionic liquids and ionic liquid mixtures
F. Maier, T. Cremer, C. Kolbeck, K. R. J. Lovelock, N. Paape, P. S. Schulz, P. Wasserscheid and H.-P. Steinrück, *Phys. Chem. Chem. Phys.*, 2010, **DOI:** 10.1039/b920804f

Ionic liquids and reactive azeotropes: the continuity of the aprotic and protic classes
José N. Canongia Lopes and Luís Paulo N. Rebelo, *Phys. Chem. Chem. Phys.*, 2010, **DOI:** 10.1039/b922524m

A COSMO-RS based guide to analyze/quantify the polarity of ionic liquids and their mixtures with organic cosolvents
José Palomar, José S. Torrecilla, Jesús Lemus, Víctor R. Ferro and Francisco Rodríguez, *Phys. Chem. Chem. Phys.*, 2010, **DOI:** 10.1039/b920651p

Solid and liquid charge-transfer complex formation between 1-methylnaphthalene and 1-alkyl-cyanopyridinium bis{(trifluoromethyl)sulfonyl}imide ionic liquids
Christopher Hardacre, John D. Holbrey, Claire L. Mullan, Mark Nieuwenhuyzen, Tristan G. A. Youngs, Daniel T. Bowron and Simon J. Teat, *Phys. Chem. Chem. Phys.*, 2010, **DOI:** 10.1039/b921160h

Blending ionic liquids: how physico-chemical properties change
F. Castiglione, G. Raos, G. Battista Appetecchi, M. Montanino, S. Passerini, M. Moreno, A. Famulari and A. Mele, *Phys. Chem. Chem. Phys.*, 2010, **DOI:** 10.1039/b921816e

NMR spectroscopic studies of cellobiose solvation in EmimAc aimed to understand the dissolution mechanism of cellulose in ionic liquids
Jinming Zhang, Hao Zhang, Jin Wu, Jun Zhang, Jiasong He and Junfeng Xiang, *Phys. Chem. Chem. Phys.*, 2010, **DOI:** 10.1039/b920446f

Electrochemical carboxylation of α-chloroethylbenzene in ionic liquids compressed with carbon dioxide
Yusuke Hiejima, Masahiro Hayashi, Akihiro Uda, Seiko Oya, Hiroyuki Kondo, Hisanori Senboku and Kenji Takahashi, *Phys. Chem. Chem. Phys.*, 2010, **DOI:** 10.1039/b920413j

A theoretical study of the copper(I)-catalyzed 1,3-dipolar cycloaddition reaction in dabco-based ionic liquids: the anion effect on regioselectivity
Cinzia Chiappe, Benedetta Mennucci, Christian Silvio Pomelli, Angelo Sanzone and Alberto Marra, *Phys. Chem. Chem. Phys.*, 2010, **DOI:** 10.1039/b921204c

Fragility, Stokes–Einstein violation, and correlated local excitations in a coarse-grained model of an ionic liquid
Daun Jeong, M. Y. Choi, Hyung J. Kim and YounJoon Jung, *Phys. Chem. Chem. Phys.*, 2010, **DOI:** 10.1039/b921725h

Reactions of excited-state benzophenone ketyl radical in a room-temperature ionic liquid
Kenji Takahashi, Hiroaki Tezuka, Shingo Kitamura, Toshifumi Satoh and Ryuzi Katoh, *Phys. Chem. Chem. Phys.*, 2010, **DOI:** 10.1039/b920131a

In search of pure liquid salt forms of aspirin: ionic liquid approaches with acetylsalicylic acid and salicylic acid
Katharina Bica, Christiaan Rijksen, Mark Nieuwenhuyzen and Robin D. Rogers, *Phys. Chem. Chem. Phys.*, 2010, **DOI:** 10.1039/b923855g

Nanocomposites of ionic liquids confined in mesoporous silica gels: preparation, characterization and performance
Juan Zhang, Qinghua Zhang, Xueli Li, Shimin Liu, Yubo Ma, Feng Shi and Youquan Deng, *Phys. Chem. Chem. Phys.*, 2010, **DOI:** 10.1039/b920556j

An ultra high vacuum-spectroelectrochemical study of the dissolution of copper in the ionic liquid (*N*-methylacetate)-4-picolinium bis(trifluoromethylsulfonyl)imide
Fulian Qiu, Alasdair W. Taylor, Shuang Men, Ignacio J. Villar-Garcia and Peter Licence, *Phys. Chem. Chem. Phys.*, 2010, **DOI:** 10.1039/b924985k

Understanding siloxane functionalised ionic liquids
Heiko Niedermeyer, Mohd Azri Ab Rani, Paul D. Lickiss, Jason P. Hallett, Tom Welton, Andrew J. P. White and Patricia A. Hunt, *Phys. Chem. Chem. Phys.*, 2010, **DOI:** 10.1039/b922011a

On the electrodeposition of tantalum from three different ionic liquids with the bis(trifluoromethyl sulfonyl) amide anion
Adriana Ispas, Barbara Adolphi, Andreas Bund and Frank Endres, *Phys. Chem. Chem. Phys.*, 2010, **DOI:** 10.1039/b922071m

Solid-state dye-sensitized solar cells using polymerized ionic liquid electrolyte with platinum-free counter electrode
Ryuji Kawano, Toru Katakabe, Hironobu Shimosawa, Md. Khaja Nazeeruddin, Michael Grätzel, Hiroshi Matsui, Takayuki Kitamura, Nobuo Tanabec and Masayoshi Watanabe, *Phys. Chem. Chem. Phys.*, 2010, **DOI:** 10.1039/b920633g

Dynamics of ionic liquid mediated quantised charging of monolayer-protected clusters
Stijn F. L. Mertens, Gábor Mészáros and Thomas Wandlowski, *Phys. Chem. Chem. Phys.*, 2010, **DOI:** 10.1039/b921368f

Insights into the surface composition and enrichment effects of ionic liquids and ionic liquid mixtures

F. Maier,*[a] T. Cremer,[a] C. Kolbeck,[a] K. R. J. Lovelock,[b] N. Paape,[c] P. S. Schulz,[c] P. Wasserscheid[c] and H.-P. Steinrück[a]

Received 5th October 2009, Accepted 4th December 2009
First published as an Advance Article on the web 9th January 2010
DOI: 10.1039/b920804f

A systematic study of ionic liquid surfaces by angle resolved X-ray photoelectron spectroscopy (ARXPS) is presented. By reviewing recent and presenting new results for imidazolium-based ionic liquids (ILs), we discuss the impact of chemical differences on surface composition and on surface enrichment effects. (1) For the hydrophilic ethylene glycol (EG) functionalised ILs [Me(EG)MIm][Tf_2N], [Et(EG)$_2$MIm][Tf_2N] and [Me(EG)$_3$MIm][Tf_2N], which vary in the number of ethylene glycol units (from 1 to 3), we find that the surface composition of the near-surface region is in excellent agreement with the bulk composition, which is attributed to attractive interactions between the oxygen atoms on the cation to the hydrogen atoms on the imidazolium ring. (2) For [C_nC_1Im][Tf_2N] (where n = 1–16), *i.e.* ILs with an alkyl chain of increasing length, an enrichment of the aliphatic carbons is observed for longer chains ($n > 2$), at the expense of the polar cation head groups and the anions in the first molecular layer, both of which are located approximately at the same distance from the outer surface. (3) To study the influence of the anion on the surface enrichment, we investigated ten ILs [C_8C_1Im][X] with the same cation, but very different anions $[X]^-$. In all cases, surface enrichment of the cation alkyl chains is found, with the degree of enrichment decreasing with increasing size of the anion, *i.e.*, it is most pronounced for the smallest anions and least pronounced for the largest anions. (4) For the IL mixture [C_2C_1Im][Tf_2N] and [$C_{12}C_1$Im][Tf_2N] we find a homogeneous distribution in the outermost surface region with no specific enrichment of the $[C_{12}C_1Im]^+$ cation.

1. Introduction

Ionic liquids (ILs) belong to the materials class of molten salts and have—per definition—a melting point below 100 °C. Over more than a decade they have received strongly increasing scientific attention.[1] This high interest is due to their structural diversity (one might think of more than 10^6 different ILs) and their unique physico-chemical properties such as unusual solvation and miscibility properties,[2] large electrochemical window, extremely low volatility,[3,4] their electroconductivity,[5] *etc*. These properties open manifold routes to applications in catalysis,[6] electrochemistry,[5] analytics,[7] and as "engineering fluids" (*e.g.* in separation technologies[8]), some of which have been already adopted by industry.[9] The properties of ILs can be tuned over a wide range by introducing alkyl chains or functional groups at the cation or the anion, thereby adapting them to specific applications. In the context of this concept the term "task specific ionic liquids" (TSILs) has been coined.[1,10]

The "bulk" properties (*e.g.*, liquid range, density, coordination behaviour, heat capacity, polarity, viscosity) of common ILs have received considerable attention in the past; in contrast, "ionic liquid surface science", *i.e.*, the investigation of their surface and interface properties just started a few years ago.[11–13] The increasing interest in this field is due to the importance of the interface of an IL with its environment (solid, liquid or gaseous) in a large number of application areas (see ref. 14–16 and references therein). In order to explain fundamental macroscopic surface properties such as surface tension,[17] electron transfer processes in electrochemistry,[5,18] or the application in multiphase catalysis (*e.g.*, "supported ionic liquid phase (SILP)" catalysis[19–21]), an understanding of the liquid–vapour interface on a molecular level is vital. Due to the unbalanced forces which are present as a result of the non-isotropic environment, the chemical composition of the near-surface region and the molecular arrangement at the surface can be different to that in the bulk.

Due to the very low vapour pressure of ILs[22–24] the complete toolbox of surface science methods can be applied to investigate IL surfaces with atomic-level accuracy under ultra-high vacuum (UHV). These methods include direct recoil spectroscopy (DRS),[11,12] high resolution electron energy loss spectroscopy (HREELS),[25] low energy ion scattering (LEIS),[26] and Rutherford backscattering.[27] In addition, other

[a] *Lehrstuhl für Physikalische Chemie II, Department Chemie und Pharmazie, Friedrich-Alexander-Universität Erlangen-Nürnberg, Egerlandstraße 3, 91058 Erlangen, Germany. E-mail: florian.maier@chemie.uni-erlangen.de*
[b] *School of Chemistry, The University of Nottingham, University Park, Nottingham, UK NG7 2RD*
[c] *Lehrstuhl für Chemische Reaktionstechnik, Department Chemie- und Bioingenieurwesen, Friedrich-Alexander-Universität Erlangen-Nürnberg, Egerlandstraße 3, 91058 Erlangen, Germany*

surface sensitive methods without UHV requirements such as sum frequency generation (SFG),[15,28–33] X-ray and neutron reflectometry,[33–35] surface tension measurements,[17,31,36–38] grazing incidence X-ray diffraction[39] and simulations[40–43] have also been applied.

XPS, also denoted as electron spectroscopy for chemical analysis (ESCA), is one of the most powerful UHV methods to analyse the chemical composition of the near-surface region of condensed matter. Since the core level binding energies are sensitive to the local chemical environment, resulting in the so-called chemical shift, one can also determine the chemical state (*e.g.*, oxidation state) of a particular atom. XPS is inherently surface sensitive due to the low inelastic mean free path of photoelectrons (a few to ten atomic layers, depending on the kinetic energy and material),[44] which can be employed to determine the composition depth profiles of the near-surface region.[45] While XPS is commonly performed under ultrahigh vacuum (UHV) conditions (pressures below 10^{-6} mbar) and restricted to solid surfaces, the negligible vapour pressure of ILs at room temperature ($<10^{-9}$ mbar) opens up the possibility to also study liquid surfaces and to determine their properties in great detail.

After pioneering XPS studies were applied on ILs in 2005,[46] investigations under different experimental conditions on numerous neat, functionalised ILs, and on IL solutions have demonstrated that XPS is indeed a very powerful tool to study IL surfaces.[26,46–58] Recently, an angle resolved XPS (ARXPS) investigation demonstrated the potential of ARXPS to derive conclusions on the enrichment of alkyl chains at the liquid/vacuum interface.[53] Furthermore, it was shown particularly by our own work that the composition of the IL in the near-surface region can be quantified with high accuracy,[54,55] and surface contaminants[50,54] and surface enrichment effects[51,56–58] can be determined by ARXPS.

The present study addresses the surface composition of hydrophilic polyethylene glycol (PEG) functionalised ILs, ILs with hydrophobic alkyl chains with a varying chain length and combined with different anions, and, to our knowledge for the first time, mixtures of ionic liquids, by XPS. Mixtures are of particular interest, because variations in the composition allow for a subtle tuning of IL properties.[59] In all cases presented here the cation contains an imidazolium ring, and for the majority of ILs the anion is bis[(trifluoromethyl)sulfonyl]imide ($[Tf_2N]^-$); only when the influence of the nature of the anion on the alkyl surface enrichment is investigated, the type of anion is systematically varied. The present study reconciles results, which have been published by us recently[54,57,58] together with a set of new data, with particular emphasis on (1) surface enrichment and orientation effects for functional chains and alkyl chains attached to the imidazolium ring in the cation, (2) the influence of the nature of the anion on this behaviour and, (3) surface enrichment effects in binary IL mixtures. For each IL all relevant core levels were investigated (see also ref. 54, 57, 58); however, the conclusions derived here are mainly based on the spectra of the C 1s region and therefore mostly C 1s data are presented. If relevant or necessary, also the results from other spectral regions are discussed.

2. Experimental

The synthesis and characterization of the different ionic liquids investigated in this study have been reported in previous publications;[57,58] a summary of the investigated pure ILs is given in Table 1. IL mixtures were prepared in defined molar ratios by stirring the required masses of ILs in excess of dichloromethane for 1 h and by subsequent removal of the volatile solvent under vacuum conditions. Thin IL films were prepared by deposition of the corresponding IL onto a planar, precleaned Au foil (10 × 10 × 0.1 mm). Immediately thereafter, these samples were introduced in the ultra-high vacuum (UHV) system *via* a loadlock (exposure time to air during transfer <1 min). After at least 6 h of pumping, the pressure was $\sim 5 \times 10^{-10}$ mbar, hardly exceeding the base pressure in the vacuum system; this low pressure also confirms the very low vapour pressure of the ionic liquid and the absence of volatile impurities. It is important to note that due to careful synthesis and cleaning of the ILs prior to transfer into our vacuum system, none of the investigated ILs showed any sign of surface contaminations, which can present a major problem when investigating the IL surfaces.[46,50,54]

The XPS measurements were performed with an ESCALAB 200 system using Al Kα radiation ($h\nu$ = 1486.6 eV); the spectra were collected with a pass energy of 20 eV, yielding an overall energy resolution of 0.9 eV. The Au $4f_{7/2}$ signal (E_B = 83.55 eV) was used as a reference for the reported binding energies. ILs, however, have been shown to charge, even for low viscosity ILs.[57] Under the experimental conditions of the XPS setup in use, peak positions were reproduced with variations of about ±0.15 eV.[57] No significant beam damage occurred over the time scale of the ARXPS experiments reported here.

To vary the surface sensitivity of the measurements, spectra were collected under $\theta = 0°$ (normal emission) and for $\theta = 70°$ and 80° (grazing emission). Due to the small acceptance angle of ±4° of the electron analyser, the probe depth varies mainly with $\cos(\theta)$. Considering the inelastic mean free path of ~3 nm of photoelectrons in organic compounds[60] at the kinetic energies used (~800–1300 eV), measurements at $\theta = 0°$ probe the near-surface region (information depth, ID: 7–9 nm, depending on the kinetic energy); measurements at 70° (ID: 2–3 nm), and 80° (ID: 1–1.5 nm) probe the topmost surface layers. At 80°, 65% of the XPS intensity arises from the first 0.3–0.5 nm, which is below the size of most of the IL ions studied herein. This high surface sensitivity allows one to derive information on the surface composition and on the arrangement of the molecules in the topmost layer.

To correct for reduced overall transmission, the spectra recorded at 70 and 80° were multiplied by an empirical constant determined by measurements of an IL comprised of small ions. As in our previous studies, $[C_2C_1Im][Tf_2N]$ was selected as the reference substance.[54] For cross-checking, a clean gold foil was also used. Thus, for a homogenous distribution of the various elements in the investigated sample, identical signals are expected at all emission angles. In contrast, an increase in core level intensity with increasing detection angle and, thus, with increasing surface sensitivity, indicates a

Table 1 Summary of ILs investigated in this study

Chemical Formula	Structure	Name
[Me(EG)MIm][Tf_2N]	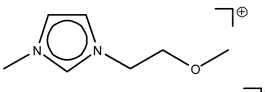	3-[2-methoxy-ethyl]-1-methylimidazolium bis[(trifluoromethyl)sulfonyl]imide
[Et(EG)$_2$MIm][Tf_2N]	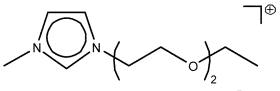	3-[2-(2-ethoxy-ethoxy)-ethyl]-1-methylimidazolium bis[(trifluoromethyl)sulfonyl]imide
[Me(EG)$_3$MIm][Tf_2N]	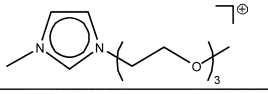	3-[2-(2-(2-methoxy-ethoxy)-ethoxy)-ethyl]-1-methylimidazolium bis[(trifluoromethyl)sulfonyl]imide
[C_nC_1Im][Tf_2N] (n = 1,2,4,6,8,10,12,16)	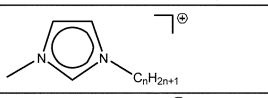	1-alkyl-3-methylimidazolium bis[(trifluoromethyl)sulfonyl]imide
[C_8C_1Im]Cl	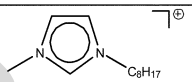	1-octyl-3-methylimidazolium chloride
[C_8C_1Im]Br	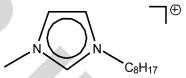	1-octyl-3-methylimidazolium bromide
[C_8C_1Im]I	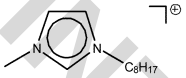	1-octyl-3-methylimidazolium iodide
[C_8C_1Im][NO_3]	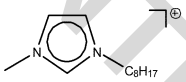	1-octyl-3-methylimidazolium nitrate
[C_8C_1Im][BF_4]	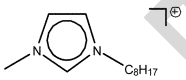	1-octyl-3-methylimidazolium tetrafluoroborate
[C_8C_1Im][PF_6]	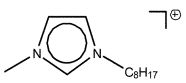	1-octyl-3-methylimidazolium hexafluorophosphate
[C_8C_1Im][TfO]	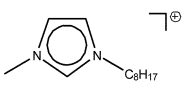	1-octyl-3-methylimidazolium trifluoromethylsulfonate
[C_8C_1Im][Pf_2N]	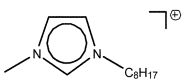	1-octyl-3-methylimidazolium bis[(pentafluoroethyl)sulfonyl]imide
[C_8C_1Im][FAP]	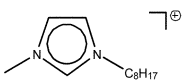	1-octyl-3-methylimidazolium tris(pentafluoroethyl)trifluoro-phosphate

higher concentration of this element in the topmost layers as compared to the bulk. This, in principle, can be due to the surface enrichment of a contamination,[50] of one component in a mixture or solution of ILs[51] or due to a pronounced preferential orientation of cations or anions in the IL.[57,58]

For C 1s spectra of ILs with CF_3-groups, a three point linear background subtraction was applied, for all other spectra a two point linear background subtraction was used. All peaks were fitted using Gaussian lineshapes. Using the areas under the fitted peaks and taking into account the sensitivity factors for the different elements, quantitative information was obtained on the stoichiometry of the near-surface region. The atomic sensitivity factors (ASFs) used are those reported by Kolbeck *et al.* for our specific experimental setup.[54,58]

3. Results and discussion

3.1 Hydrophilic PEG-functionalised IL: [Me(EG)$_3$MIm][Tf_2N]

In order to investigate possible orientation effects for long functionalised chains at the IL cation, we studied [Me(EG)$_3$MIm][Tf_2N], a PEG IL containing three ethylene glycol functionalities in the cation alkyl chain using ARXPS. The structure of this IL is given in Fig. 1, along with the corresponding C 1s (a) and F 1s (b) XP spectra at emission angles of 0, 70 and 80°. Focussing on the C 1s spectra first, the peak at 292.8 eV is assigned to the C atoms in the anion (C_{anion}) the peaks at 286.6 eV to the C atoms in the cation (C_{cation}); note that both the C atoms in the imidazolium ring and in the ethylene glycol units have neighbouring hetero

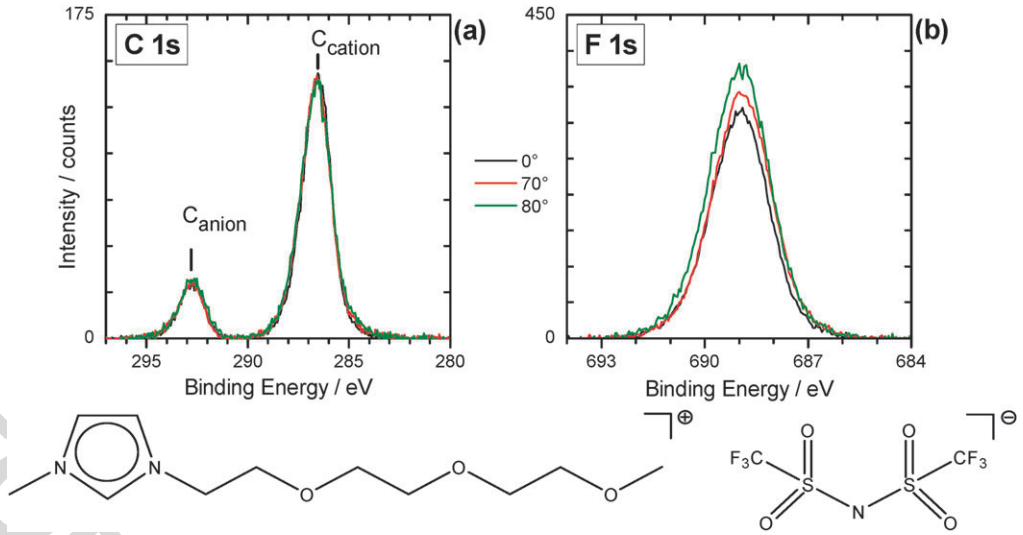

Fig. 1 XP spectra of $[Me(EG)_3MIm][Tf_2N]$, recorded under 0° (black), 70° (red) and 80° (green) electron emission angles, with respect to the surface normal: (a) C 1s region, (b) F 1s region.

atoms (N or O, respectively) and consequently exhibit very similar binding energies, which cannot be resolved with our setup. The corresponding peak C_{cation} was thus successfully fitted with one component only for all C 1s spectra here (see also Kolbeck *et al.*[54]) in contrast to ILs containing aliphatic carbon atoms (see next section).

Detailed spectra have also been measured for the O 1s, N 1s, and S 2p regions (not shown). Briefly, in the O 1s spectra only one peak is observed at 532.7 eV which is attributed to the EG oxygen atoms from the cation and the sulfoxy oxygen atoms from the anion, which coincidentally have the same binding energies; in the N 1s region two peaks are found at 401.9 and 399.2 eV which are assigned to the N atoms in the cation and anion, respectively; the F 1s (shown in Fig. 1b) and spin–orbit split S 2p levels are found at 688.9 and 168.8 eV (S $2p_{3/2}$), respectively. The normalised intensity ratios of the peaks in the (bulk sensitive) normal emission spectra are: $C_{anion}:C_{hetero}:N_{anion}:N_{cation}:O:F:S = 2.1(2.0):11.2(11.0):1.1(1.0):2.1(2.0):6.9(7.0):5.7(6.0):2.0(2.0)$ (see also Table 2). The comparison to the nominal composition (values in brackets) shows excellent agreement within the margin of error of ~10%, confirming the chemical composition of the IL on one hand, and the accuracy of the measurement on the other hand.

The C 1s spectra for the different angles (0, 70 and 80°) in Fig. 1a show identical line shapes and intensities, indicative of a homogeneous distribution of the C atoms in the near-surface region and in the bulk. Similar agreement is also observed for the O 1s and S 2p spectra. However, the F 1s spectra in Fig. 1b show an enhancement by about 10% at 80° (increased surface sensitivity) indicating a greater amount of fluorine in the very near-surface region than expected by stoichiometry. Furthermore, there was also a decrease of cation N signal intensity by about 10% upon increasing the emission angle to 80° (see Table 2). This result is in line with high resolution Rutherford backscattering measurements for $[N(Me)_3Pr][Tf_2N]$, which show that fluorine atoms are located at the outer surface.[27] Thus, we conclude for the PEG ILs studied here that in the near-surface region cations and anions are homogeneously distributed and randomly oriented, with no enrichment of the EG-functionalised hydrophilic alkyl chain at the outer surface. The anions in the first surface layer are preferentially oriented in such a way that the F atoms are slightly enriched at the outermost surface which is most likely due to the non-coordination nature of CF_3-groups in general.

Similar results were also observed for ILs containing only one or two ethylene glycol functionalities in the cation alkyl chain, namely $[Me(EG)MIm][Tf_2N]$ and $[Et(EG)_2MIm][Tf_2N]$.[54] Again, the experimentally determined chemical compositions correspond excellently with the nominal values and the C 1s ARXPS data indicate a homogeneous distribution of the C atoms in the bulk and near-surface region, with some preferential enrichment of fluorine at the outer surface. The fact that, independent of the length of the hydrophobic functionalised

Table 2 Quantitative analysis of the XP spectra of $[Me(EG)_3MIm][Tf_2N]$[a]

	N 1s (ring)	N 1s (anion)	C 1s (cation)	O 1s	F 1s	S 2p	C 1s (anion)
Position peak maxima/eV	401.9	399.3	286.6	532.8	689.0	168.8	292.8
Nominal	2.0	1.0	11.0	7.0	6.0	2.0	2.0
0°	2.1	1.1	11.2	6.9	5.7	2.0	2.1
70°	1.9	1.0	11.0	6.9	6.2	2.0	2.1
80°	1.7	1.0	10.8	6.7	6.9	1.9	2.2

[a] The nominal and the experimentally determined compositions in number of atoms are given for the various elements constituting the IL; the experimental values are derived from XP spectra at 0, 70 and 80°. The atomic sensitivity factors (ASF) taking the transmission function of our electron analyser into account are taken from ref. 54.

chain, no orientation effect or surface enrichment of the chain is observed appears surprising at first sight.

In the following, we provide some interpretation for these findings. From measurements of the melting points for a number of ether-functionalised imidazolium ILs it has been concluded that the lattice energy for ethylene glycol functionalised ILs is larger than for comparable systems without EG units. This behaviour was attributed to additional attractive interactions between the EG oxygen on the cation and hydrogen atoms of either the cation or anion. Using IR spectroscopy and density functional theory Fei *et al.* showed for EG-functionalised halide ILs that a hydrogen-bonding type interaction indeed exists between the oxygen atoms on the functionalised chain and the hydrogen atoms on the imidazolium ring, especially the electropositive hydrogen in 2-position of the imidazolium ring.[61] Recent molecular dynamics simulations have also shown attractive interactions between the oxygen of a cation based side-chain and the hydrogen atoms of the imidazolium ring, both intra- and intermolecularly.[62] Hydrogen bonding between the oxygen atoms in the functionalised chain on the cation to the hydrogen atoms on the imidazolium ring would make an enrichment of the chains at the surface energetically unfavourable; consequently, the outer surface is preferentially composed of the anions non-coordinating CF_3 groups rather than any groups from the cation.

3.2 Hydrophobic non-functionalised ILs: $[C_nC_1Im][Tf_2N]$

As a next step we address the composition of the near-surface region of eight non-functionalised imidazolium ionic liquids of type $[C_nC_1Im][Tf_2N]$. To systematically investigate the role of the alkyl chain, its length was varied from $n = 1$ to 16. XPS signals were observed for all expected elements.[57] Fig. 2 shows the C 1s (a) and the N 1s (b) XP spectra at normal emission (0°) for $[C_nC_1Im][Tf_2N]$. In the C 1s spectra three peaks are observed; the peak at around 292.5 eV (labelled as '3') is assigned to the C atoms (C_{anion}) in the $[Tf_2N]^-$ anion, as for the $[Tf_2N]^-$ containing PEG ILs of the previous section. The peaks at lower binding energies are assigned to the carbon atoms with different chemical environments in the cation: the peak at around 286.5 eV is assigned to carbon atoms, which have hetero atoms (N) as neighbours (see also section 3.1.) and therefore is denoted as C_{hetero}; the peak at 284.8 eV is assigned to C atoms with exclusively carbon (or hydrogen) neighbours[53,57,58] and is denoted as C_{alkyl}. Note that for $[C_1C_1Im][Tf_2N]$ containing only hetero bonded carbon, C_{alkyl} is absent which results in a symmetric C_{hetero} signal in the C 1s region and, thus, corroborates the peak assignments. Fitting of the two carbon signals provided very reliable results when employing only one empirically derived constraint for the full-width-at-half-maximum (FWHM) values, namely $FWHM(C_{hetero}) = FWHM(C_{alkyl}) \times 1.11$. The corresponding N 1s spectra shown in Fig. 2b exhibit two signals: the peak at 402 eV corresponds to the two nitrogen atoms in the imidazolium ring whereas the peak at 399 eV is attributed to the nitrogen of the $[Tf_2N]^-$ anion.[54,57] The slight overall shift of the spectra towards higher binding energies with increasing n, and, thus, with increasing viscosity, is attributed either to subtle charging effects and/or changes in the work function. As explained earlier,[57] the shift for C_{alkyl} is compensated by the fact that for rather small chains ($n < 8$) carbon atoms closer to the ring exhibit a higher binding energy than carbon atoms near the end of the chain.

The quantitative analysis of all IL signals in the bulk sensitive geometry (*i.e.*, at an electron emission angle of 0°, which corresponds to an information depth of ~7–9 nm, depending on kinetic energy) is given in Table 3. It shows that the experimentally determined composition agrees with the nominal one to a very high level of accuracy (in most cases better than 5%). *E.g.*, for $n = 8$ ($[C_8C_1Im][Tf_2N]$) the normalised intensity ratios are: $C_{anion} : C_{hetero} : C_{alkyl} : N_{anion} : N_{cation} : O : F : S = 2.1(2.0) : 5.0(5.0) : 7.1(7.0) : 1.0(1.0) : 2.1(2.0) : 3.9(4.0) : 5.9(6.0) : 2.0(2.0)$ with the values in brackets again indicating the nominal composition.

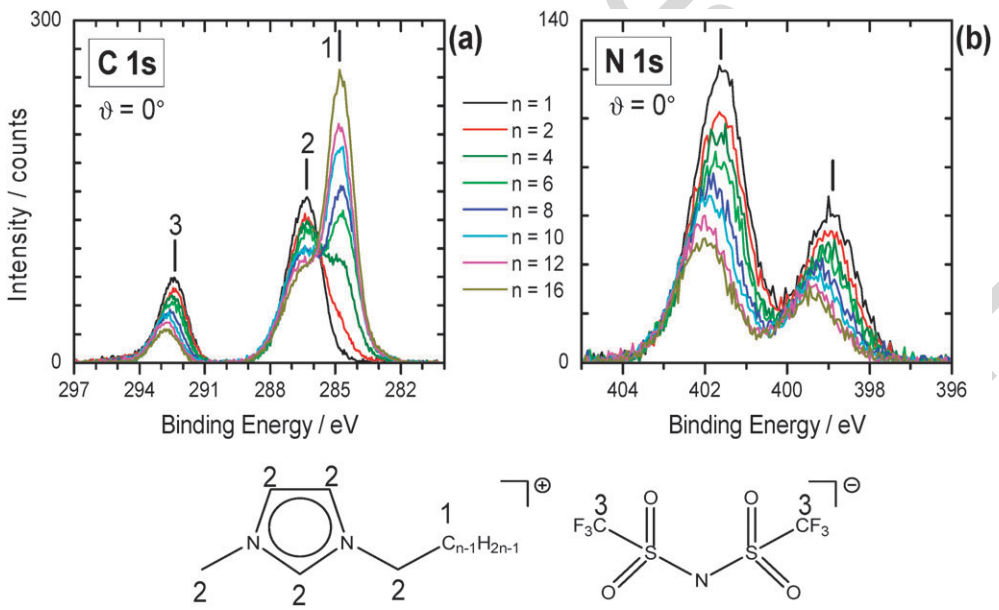

Fig. 2 C 1s (a) and N 1s (b) XP spectra of $[C_nC_1Im][Tf_2N]$ (where n = 1–16), recorded under 0° electron emission angle.

Table 3 Quantitative analysis of the XP spectra of $[C_nC_1Im][Tf_2N]$. The nominal and the experimentally determined compositions in the number of atoms are given for the various elements constituting the ILs; the experimental values are derived from XP spectra taken at 0°. The atomic sensitivity factors (ASF) taking the transmission function of our electron analyser into account are taken from Kolbeck *et al.*[54]

		C 1s (hetero)	C 1s (alkyl)	N 1s (cation)	C 1s (anion)	N 1s (anion)	O 1s (anion)	S 2p (anion)	F 1s (anion)
Position peak maxima/eV		286.6	284.8	401.9	292.7	399.3	532.5	168.8	688.8
ASF		0.205	0.205	0.350	0.205	0.350	0.580	0.400	1.000
$[C_1C_1Im][Tf_2N]$	Nominal	5.0	0.0	2.0	2.0	1.0	4.0	2.0	6.0
	0°	4.9	<0.1	2.0	2.1	1.0	4.0	2.0	6.0
$[C_2C_1Im][Tf_2N]$	Nominal	5.0	1.0	2.0	2.0	1.0	4.0	2.0	6.0
	0°	5.1	0.8	2.1	2.1	1.0	4.0	2.0	5.9
$[C_4C_1Im][Tf_2N]$	Nominal	5.0	3.0	2.0	2.0	1.0	4.0	2.0	6.0
	0°	5.1	3.1	2.1	2.1	1.0	3.9	2.1	5.8
$[C_6C_1Im][Tf_2N]$	Nominal	5.0	5.0	2.0	2.0	1.0	4.0	2.0	6.0
	0°	5.2	5.2	2.0	2.0	1.0	3.8	2.0	5.8
$[C_8C_1Im][Tf_2N]$	Nominal	5.0	7.0	2.0	2.0	1.0	4.0	2.0	6.0
	0°	5.1	7.0	2.1	2.0	1.0	3.9	2.0	5.9
$[C_{10}C_1Im][Tf_2N]$	Nominal	5.0	9.0	2.0	2.0	1.0	4.0	2.0	6.0
	0°	5.4	9.2	2.0	2.0	1.0	3.8	2.0	5.7
$[C_{12}C_1Im][Tf_2N]$	Nominal	5.0	11.0	2.0	2.0	1.0	4.0	2.0	6.0
	0°	5.5	11.8	2.0	1.9	1.0	3.9	1.9	5.5
$[C_{16}C_1Im][Tf_2N]$	Nominal	5.0	15.0	2.0	2.0	1.0	4.0	2.0	6.0
	0°	5.7	15.5	2.0	1.8	1.0	3.7	1.9	5.5

If we compare the spectra by increasing chain length n, we find that the C_{alkyl} peak at 284.8 eV increases in intensity with increasing chain length, as expected from the increasing number of alkyl chain atoms (see also Table 1). Simultaneously, the intensities of all other IL signals decrease with increasing chain length as shown for the C_{anion}, C_{hetero} and N 1s signals in Fig. 2. This decrease is attributed to the fact that with increasing chain length the size (volume) of the individual cation increases and, therefore, the molar density of the cation/anion pairs decreases. As XPS measures the number of molecules per volume, the XP signal has to decrease if the density decreases, which is exactly what is observed.[54] To visualise the quantitative analysis, we have plotted the intensity ratios of the C_{alkyl} signal and the C_{hetero} signal as a function of chain length n in Fig. 3g for the normal emission spectra (black symbols). The data points show excellent agreement with the values expected from the nominal composition (dashed line).

In order to identify possible enrichment effects, we analysed the XP spectra at grazing emission, *i.e.* in the surface sensitive geometry at $\theta = 80°$ with an I.D. of 1–1.5 nm. The corresponding C 1s spectra for chain length of $n = 1$, 8 and 16, are shown in Fig. 3. For $[C_1C_1Im][Tf_2N]$ very little changes were observed with a changed emission angle, similar to the PEG functionalised ILs (see section 3.1), indicating a homogenous distribution and orientation of the ions at the surface. However, for $[C_8C_1Im][Tf_2N]$ and $[C_{16}C_1Im][Tf_2N]$, pronounced differences are found. Upon increasing the emission angle, the intensity of the C_{alkyl} peak increases and simultaneously the intensities of the C_{anion} and C_{hetero} peaks (and also that of the N_{cation} and N_{anion} peaks as shown in Fig. 3) decrease. This behaviour clearly indicates that the alkyl chains are enriched in the near-surface region and the anion and hetero carbon atoms as well as the nitrogen atoms are depleted. The enhancement of the C_{alkyl} signal and the decrease in the other signals is more pronounced for $[C_{16}C_1Im][Tf_2N]$ than for $[C_8C_1Im][Tf_2N]$, indicating that the enrichment is stronger for the IL with the longer alkyl chain.

As a measure of the surface enrichment we can again use the ratio of the C_{alkyl} signal and the C_{hetero} signal. The corresponding data for emission angles of 0, 70, and 80° as a function of chain length are given in Fig. 3g. Clearly, the deviation from the nominal composition (dashed line) increases with emission angle, but more importantly with chain length. This is an unequivocal indication that the degree of surface enrichment of the alkyl chains increases with increasing the chain length.

Information on the relative position of the imidazolium ring of the cation and the anion can be taken from the N 1s spectra at 80°. Also, for $n = 1$–16 the ratio of $I(N_{cation}) : I(N_{anion})$ is approximately as expected for a homogeneous distribution of ions, with a tendency of the anion nitrogen to be located slightly above the imidazolium ring in the first layer.

Summarising these results, the following picture emerges: the outer surface of the ILs contains more hydrophobic alkyl carbon chains than expected based on stoichiometry, and the polar headgroups are in relatively close proximity to the $[Tf_2N]^-$ anion slightly above the imidazolium ring. There are different possibilities for the orientation of the alky chain which would be consistent with the experimental data: one extreme case would be an approximately perpendicular orientation of the chains to the surface, the other an arrangement approximately parallel to the surface. In the latter case, the first molecular layer would be characterised by a very dense alkyl overlayer of narrow vertical width above the polar headgroups which is unlikely due to steric repulsive interactions. In contrast, the first scenario would result in an alkyl overlayer of larger thickness but diluted alkyl chains which seems to be unfavourable, too, due to reduction in attractive van-der-Waals interactions between neighbouring alkyl chains. More likely is an intermediate tilt angle for the mean alkyl chain orientation in a similar manner as it is known for long-chain self-assembled monolayers.[63] However, the exact orientation of alkyl chains cannot be determined directly using ARXPS without additional assumptions concerning the ion distribution. From simulations,

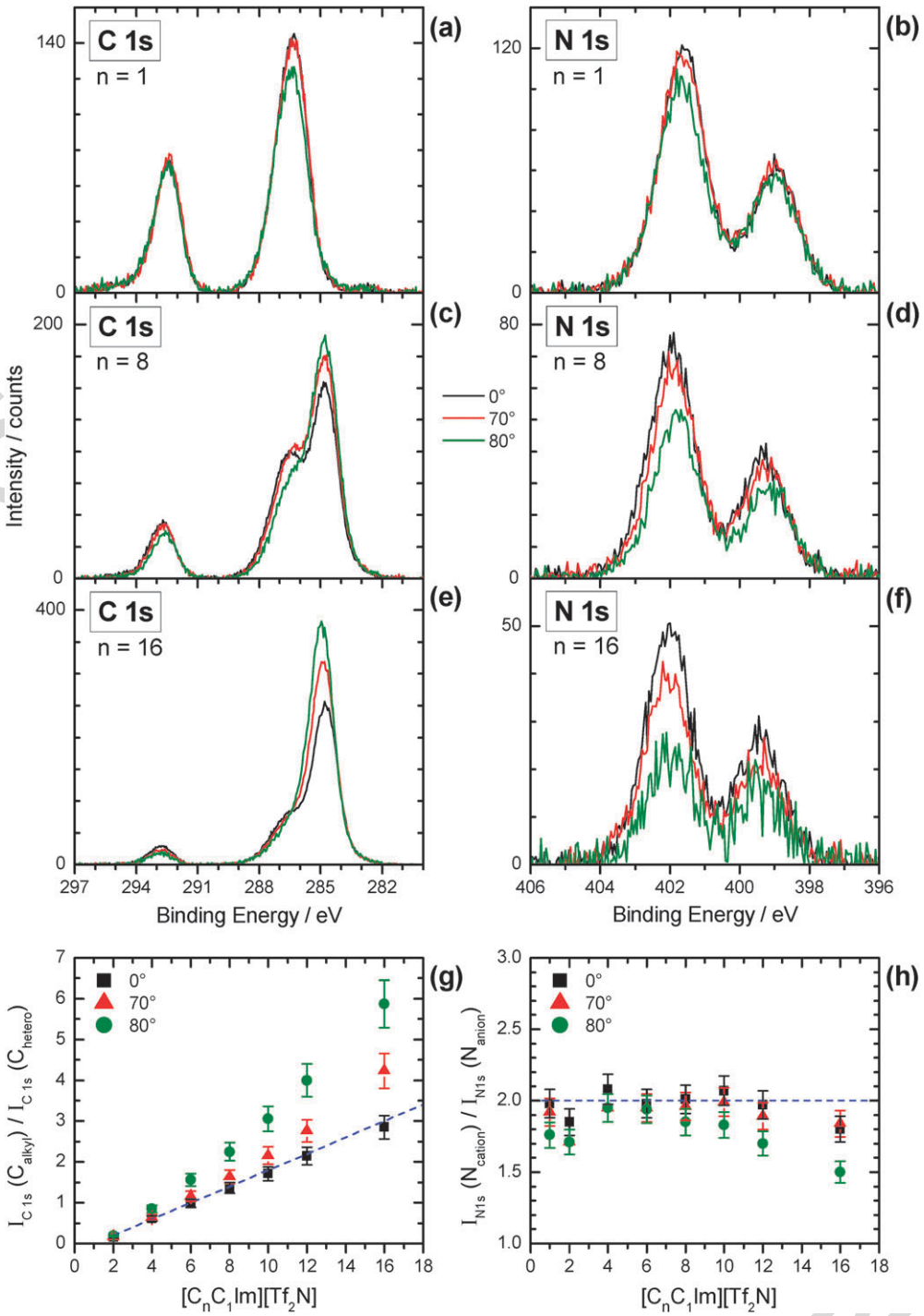

Fig. 3 (a)–(f): C 1s and N 1s XP spectra of $[C_nC_1Im][Tf_2N]$ (n = 1, 8, 16), recorded under 0° (black), 70° (red) and 80° (green) electron emission angle, with respect to the surface normal. Ratios of the intensities for $[C_nC_1Im][Tf_2N]$ recorded at different electron emission angles as a function of chain length n, (g) C_{alkyl} : C_{hetero}, (h) N_{cation} : N_{anion}. A line for the nominal ratio (blue dashed line) is also added.

Jiang *et al.* suggest that alkyl chains are oriented at ~30° to the surface normal.[40] Our results for $[C_nC_1Im][Tf_2N]$ (where n = 1–16), in terms of surface enrichment of the alkyl groups, are in good agreement with the investigation of Lockett *et al.* on $[C_nC_1Im][BF_4]$ (where n = 4–8)[53] and with findings from Baldelli *et al.* for imidazolium ILs with different alkyl chain lengths in the cation and anion.[31]

3.3 Influence of the anions: $[C_8C_1Im][X]$

In order to obtain better understanding of the factors that determine the IL surface structure, we have also studied the influence of different types of anions on the surface composition of ILs. We have investigated a large number of ILs with the same cation, 1-octyl-3-methylimidazolium $[C_8C_1Im]^+$

(see Table 1). The latter has been chosen for two main reasons. First, there is a variety of pure ILs available with this cation and very different anions which are liquid at room temperature.[23] Second, the surface enrichment of the octyl chain was already thoroughly studied for $[C_8C_1Im][Tf_2N]$ (see section 3.2). The anions $[X]^-$ in our study (see Table 1) include halides, $[NO_3]^-$, $[BF_4]^-$, $[PF_6]^-$, $[TfO]^-$ and also more complex anions containing perfluoroalkyl groups such as $[Tf_2N]^-$, $[(C_2F_5SO_2)_2N]^-$ ($[Pf_2N]^-$) or $[PF_3(C_2F_5)_3]^-$ ($[FAP]^-$); they were selected to cover different sizes (ranging from Cl^- to $[FAP]^-$), shapes (from spherical to elongated anions), and coordination abilities (from strongly coordinating halides to weakly coordinating anions with perfluoroalkyl groups).

All ten $[C_8C_1Im][X]$ ILs studied contain 12 carbon atoms solely from the common imidazolium cation, 7 C_{alkyl} atoms with the C 1s level at about 285 eV and 5 C_{hetero} atoms, located at a higher binding energy (~286.4–287.0 eV); the binding energy peak separation for C_{alkyl} and C_{hetero} depends on the nature of the anion as will be discussed elsewhere.[64] In Fig. 4, the intensity ratio $C_{alkyl}:C_{hetero}$ is plotted *vs.* the molar volume for 0 and 80° emission angle. We have chosen the molecular volume $V_M = M/\rho/N_A$ (with M, ρ, N_A being the molar mass, the mass density at room temperature and the Avogadro constant, respectively) as a convenient measure for the size of the ion pairs, as previous studies have shown that many key physicochemical properties of ILs can be directly related to this quantity.[65] The values for molecular volumes were determined from our liquid density measurements.[58]

At 0° the measured intensity ratios $C_{alkyl}:C_{hetero}$ for all ILs studied match very well the nominal ratio, 7 : 5 = 1.4, as shown in Fig. 4, where the ratio $C_{alkyl}:C_{hetero}$ (error bars: ±7%) is plotted *vs.* the molar volume (error bars: ±1.5%). This ratio indicates that within the information depth of 7–9 nm there is a homogeneous distribution of alkyl chains and imidazolium rings for all ILs, independent of the chemical nature of the anion.

Also shown in Fig. 4 are the data for an emission angle of 80°, *i.e.* an I.D. of 1.0–1.5 nm. In all cases the ratio is significantly larger than the nominal one, indicating an enrichment of the alkyl chains in the outer surface region. The intensity ratio $C_{alkyl}:C_{hetero}$ at 80° follows the trend:

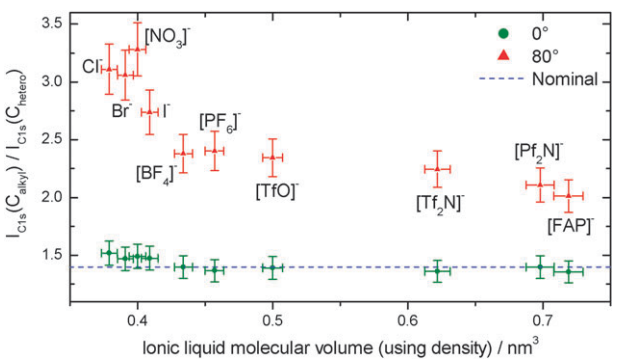

Fig. 4 Ratio of the intensities for C_{alkyl}/C_{hetero} for $[C_8C_1Im][X]$, recorded under 0° (green circles) and 80° (red triangles) electron emission angles with respect to the surface normal, against the ionic liquid molecular volume (calculated using liquid densities). A line for the nominal ratio (blue dashed line) is also added.

$Cl^- \sim Br^- \sim [NO_3]^- > I^- > [PF_6]^- \sim [BF_4]^- \sim [TfO]^- > [Tf_2N]^- > [Pf_2N]^- > [FAP]^-$ (see Table 2). The ratios clearly show that the surface enrichment of alkyl carbon relative to the ring carbon is most pronounced for the smallest anions, whereas for the largest, $[FAP]^-$, it is smallest.

In order to derive some conclusions on the anions, the anion-related signals were also investigated.[58] The intensity ratios for the central atom from the anion (B in $[BF_4]^-$, P in $[PF_6]^-$ and $[FAP]^-$, S in $[TfO]^-$, N in $[NO_3]^-$, $[Tf_2N]^-$ and $[Pf_2N]^-$) compared to the two nitrogen atoms from the imidazolium ring (representing the centre of the polar headgroup of the cation) were analysed and for all ILs studied, the nominal ratio of 0.5 (±10%) was found. For the majority of ILs this intensity ratio shows a weak increase with increasing surface sensitivity (*i.e.* at 80°), which leads to the tentative conclusion that the mean centre of the anions in the near-surface region is located nearly at the same (or even slightly shorter) distance from the outer surface as compared to the imidazolium ring irrespective of the nature of the anion, forming a more or less confined polar layer.

Our results prove that the IL surface is terminated by the octyl chains to a different degree, depending on anion size. To explain the influence of the anion on the degree of octyl chain surface enrichment (which is related to the mean orientation of the cation at the surface) we propose that mainly the small size of the anion and the strength of the interaction between the polar groups lead to the formation of a densely packed, well oriented surface layer, *e.g.* in the case of $[C_8C_1Im]Cl$. It should be noted that the surface enrichment of the octyl chains in the case of $[NO_3]^-$ is at least as pronounced as for the smaller halide anions Cl^- and Br^- which might be related to a specific interaction of the planar $[NO_3]^-$ anion with the imidazolium ring.[64] For the larger anions, the packing density decreases and the ionic region becomes more diffuse, leading to a loss in order and also a reduced enrichment of the octyl chains at the surface.

The surface enrichment of the alkyl carbon for $[C_8C_1Im][BF_4]$ is in overall agreement with results from Lockett *et al.*[53] The smaller $C_{alkyl}:C_{hetero}$ ratio at 80° in their study (about 1.9 instead of 2.3 in our case) is attributed to different fitting procedures and/or different acceptance angles of the corresponding electron analyser.[54]

3.4 IL mixture: $[C_2C_1Im][Tf_2N]$ and $[C_{12}C_1Im][Tf_2N]$

It was demonstrated above that ILs containing a hydrophobic alkyl chain at the imidazolium cation show an enrichment of this alkyl chain at the outer surface, with the degree of enhancement increasing with the length of the alkyl chain. Now the question arises, what will happen for a mixture of IL with the same anion but cations with alkyl chains of different length. One might expect a preferential enrichment of the cations with the longer chains acting like surfactants.[66] One indication of preferential enrichment is given by surface tension values (*i.e.* the surface free energy) of $[C_nC_1Im][Tf_2N]$ by our group[67] and others:[17,22,37] the longer the alkyl chain n of the cation the lower the surface tension, σ, of the pure IL (at RT, σ = 34.8 and 29.9 mN m^{-1} for $[C_2C_1Im][Tf_2N]$ and $[C_{12}C_1Im][Tf_2N]$, respectively.[67] To investigate this aspect, we

Table 4 Quantitative analysis of the XP spectra of $[C_8C_1Im][X]$ for the carbon atoms of the cation[a]

IL	Ratios $C_{alkyl}:C_{hetero}$ at 0°	70°	80°	Liquid density/g cm^{-3}	IL molecular volume/nm^3
$[C_8C_1Im]Cl$	1.52	2.20	3.11	1.01	0.38
$[C_8C_1Im]Br$	1.47	1.96	3.06	1.17	0.39
$[C_8C_1Im][NO_3]$	1.49	2.11	3.28	1.07	0.40
$[C_8C_1Im]I$	1.47	2.01	2.74	1.31	0.41
$[C_8C_1Im][BF_4]$	1.40	1.71	2.38	1.08	0.43
$[C_8C_1Im][PF_6]$	1.39	1.68	2.35	1.24	0.46
$[C_8C_1Im][TfO]$	1.37	1.69	2.40	1.14	0.50
$[C_8C_1Im][Tf_2N]$	1.36	1.63	2.25	1.27	0.62
$[C_8C_1Im][Pf_2N]$	1.40	1.60	2.11	1.37	0.70
$[C_8C_1Im][FAP]$	1.36	1.66	2.01	1.48	0.72

[a] The experimentally determined ratios of C_{alkyl} relative to C_{hetero} are given; the experimental values are derived from XP spectra taken at 0°, 70° and 80°. The nominal ratio $C_{alkyl}:C_{hetero}$ is 7 : 5 = 1.4 : 1. In addition, IL liquid density values (measured at room temperature) and molecular volumes (determined using liquid density) are shown.

prepared a mixture of $[C_2C_1Im][Tf_2N]$ and $[C_{12}C_1Im][Tf_2N]$ with a molar ratio of 9 : 1. We have chosen a larger fraction of $[C_2C_1Im][Tf_2N]$ deliberately, as a preferential surface segregation of $[C_{12}C_1Im][Tf_2N]$ would be easily detected due to its dominating C_{alkyl} signal of the C_{12} chains (see also Fig. 2). The reason for specifically choosing a 9 : 1 ratio was that each $[C_2C_1Im]^+$ cation contains one C_{alkyl} atom and each $[C_{12}C_1Im]^+$ cation contains 11 C_{alkyl} atoms. Therefore, the nominal amount of C_{alkyl} is $(0.9 \times 1) + (0.1 \times 11) = 0.9 + 1.1 = 2$, as shown in Table 4. Consequently, the nominal composition of the 9 : 1 mixture would be expected to give a C 1s signal of similar appearance to that for $[C_3C_1Im][Tf_2N]$ (the nominal composition with two C_{alkyl} atoms), if no preferential surface enrichment of one type of cation occurs. As shown above, we have measured spectra for $[C_2C_1Im][Tf_2N]$ and $[C_4C_1Im][Tf_2N]$ which allow for good comparison of the 9 : 1 mixture.

In Fig. 5a, C 1s spectra at 0° for 9 : 1 mixture, $[C_2C_1Im][Tf_2N]$, $[C_4C_1Im][Tf_2N]$ and $[C_{12}C_1Im][Tf_2N]$ are given. Clearly, the intensity of the C_{alkyl} peak of the mixture is larger than that of $[C_2C_1Im][Tf_2N]$ but smaller than that of $[C_4C_1Im][Tf_2N]$; in other words, it has an intensity very close to that expected for $[C_3C_1Im][Tf_2N]$, but is significantly smaller than that of $[C_{12}C_1Im][Tf_2N]$. Therefore, we conclude from the measurements in the bulk sensitive geometry at 0° (I.D. 7–9 nm) that the IL is an approximately homogeneous mixture with the expected stoichiometry within the probed near-surface region.

For the 70 and 80° measurements with increased surface sensitivity, a clear enhancement of the C_{alkyl} is observed for the mixture and the pure ILs (see Fig. 5). The degree of enhancement of C_{alkyl} for the mixture is similar to that for $[C_4C_1Im][Tf_2N]$, but much smaller than for $[C_{12}C_1Im][Tf_2N]$. We therefore conclude that in the 9 : 1 mixture, there is no preferential enrichment of $[C_{12}C_1Im][Tf_2N]$ as compared to $[C_2C_1Im][Tf_2N]$ at the outer surface. The measured surface tension value for the 9 : 1 mixture (σ = 33.6 mN m^{-1}) is considerably closer to $[C_2C_1Im][Tf_2N]$ than to the value of pure $[C_{12}C_1Im][Tf_2N]$. This independent surface property measurement indicates an ideal ion mixing behaviour in the surface region, too.

From our experimental ARXP spectra we can unambiguously rule out a surface that is solely dominated by one component of the mixture. Particularly, a surface layer that is mainly composed by the minority species $[C_{12}C_1Im][Tf_2N]$ with the outer surface formed by the dodecyl chains, is not found. At this stage an explanation for our findings requires further experiments and the help of theoretical investigations. One may speculate that the gain in surface free energy to form a surface dominated by $[C_{12}C_1Im][Tf_2N]$ (as indicated by the surface tension values) is counterbalanced by the loss in entropy and/or a loss in bulk free energy in the mixture. Temperature dependent ARXPS could help clarify this point. Finally, it should be mentioned that our results cannot rule out surface islands of $[C_{12}C_1Im][Tf_2N]$ phases

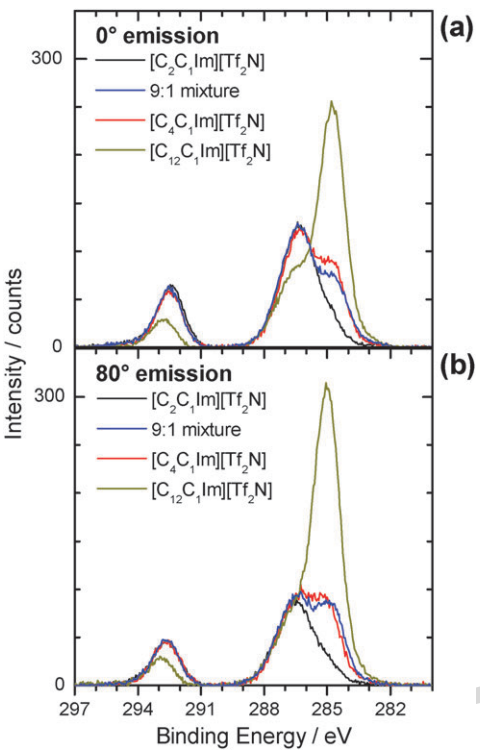

Fig. 5 9 : 1 binary mixture $[C_2C_1Im][Tf_2N]:[C_{12}C_1Im][Tf_2N]$. (a) XP spectra of C 1s region, recorded under 0° electron emission angle, with respect to the surface normal, for $[C_2C_1Im][Tf_2N]$, 9 : 1 mixture, $[C_4C_1Im][Tf_2N]$ and $[C_{12}C_1Im][Tf_2N]$. (b) XP spectra of C 1s region, recorded and 80° electron emission angle, with respect to the surface normal, for $[C_2C_1Im][Tf_2N]$, 9 : 1 mixture, $[C_4C_1Im][Tf_2N]$ and $[C_{12}C_1Im][Tf_2N]$.

separated by mixed phases, which on average yields the nominal mixture composition, since ARXPS is not sensitive to a lateral inhomogeneous distribution of molecules.

4. Summary

We present a comprehensive angle-resolved XPS study on the surface composition and surface enrichment effects of hydrophobic and hydrophilic ionic liquids and of ionic liquid mixtures, based on previous as well as on new experimental data. Such information is highly relevant for multiphase reactions occurring within ionic liquids, since the reactants have to pass the ionic liquid/vacuum (gas phase) interface. Bulk-sensitive measurements ($\theta = 0°$, information depth: 7–9 nm) and surface sensitive measurements ($\theta = 80°$, information depth: 1–1.5 nm) allow one to quantify the chemical composition of the ionic liquids and to determine surface enrichment effects of specific components. In particular, we address hydrophilic PEG functionalised ILs, ILs with hydrophobic alkyl chains of varying length, the influence of different anions, and mixtures of ionic liquids. In all cases the cation contains an imidazolium ring, and for the majority of ILs the anion is $[Tf_2N]^-$.

Hydrophilic PEG-functionalised IL

As an example for functionalised ILs, we discuss the data for $[Me(EG)_3MIm][Tf_2N]$, which contains three ethylene glycol units, and compare the results to those obtained for $[Et(EG)_2MIm][Tf_2N]$ and $[Me(EG)MIm][Tf_2N]$, with two and one EG units, respectively. In all cases we find a nearly identical chemical composition in the bulk and surface sensitive geometry, indicating a homogeneous distribution also in the near-surface region. Thus, our results indicate that the outer surfaces are similar to the bulk composition with a slight excess of fluorine from the anion, *i.e.*, CF_3 group. This behaviour is attributed to the formation of hydrogen bonds between the oxygen atoms on the cation to the hydrogen atoms on the imidazolium ring.

Hydrophobic non-functionalised ILs

To investigate the influence of the length of the alkyl chain on the cation, possible surface enrichment effects of eight non-functionalised ionic liquids $[C_nC_1Im][Tf_2N]$, with $n = 1$ to 16 were studied. The detailed analysis of the $[C_nC_1Im][Tf_2N]$ ILs unambiguously shows an enrichment of the alkyl chains at the outer surface at the expense of the imidazolium head groups and the anions. This effect monotonically increases with increasing chain length. Both anions and cationic head groups are located approximately at the same distance from the outer surface, with the anion slightly above the imidazolium ring.

Influence of the anion

Ten different ILs with the same cation $[C_8C_1Im]^+$ but anions of very different size, shape and coordination abilities were investigated. For all ILs a surface enrichment of the octyl chains in the first molecular layer is found, with the degree of enrichment decreasing with increasing anion size. It is most pronounced for Cl^-, Br^- and $[NO_3]^-$, and is considerably less prominent for the larger anions $[Pf_2N]^-$ and $[FAP]^-$. In contrast, the charged head-groups of cations and anions are located at about the same distance from the outer IL surface, forming a more or less confined polar layer. The higher degree of alkyl chain enrichment for the small anions is mainly attributed to their smaller size and stronger interaction between the polar groups which leads to the formation of a more densely packed and better oriented surface layer.

IL mixture

To investigate possible preferential enrichment effects in IL mixtures, we studied a 9 : 1 mixture of $[C_2C_1Im][Tf_2N]$ and $[C_{12}C_1Im][Tf_2N]$. The analysis of the spectra in the surface sensitive geometry clearly shows that in the binary mixture, there is no preferential enrichment of $[C_{12}C_1Im][Tf_2N]$ at the expense of $[C_2C_1Im][Tf_2N]$ at the outer surface, ruling out pronounced surfactant capabilities of long alkyl chains attached to the imidazolium ring. The question of whether alkyl chains are generally weak surfactant groups in IL systems, still needs further investigation, *e.g.* surface activity studies of catalysts containing alkyl chains of different length.

Acknowledgements

This work has been supported by the DFG through SPP1191, grants STE 620/7-2 and WA 1615/8-2 and by the Excellence Cluster "Engineering of Advanced Materials" granted to the University of Erlangen Nuremberg. We also thank the Max-Buchner-Stiftung for financial support.

References

1 *Ionic liquids in synthesis*, ed. P. Wasserscheid and T. Welton, Wiley-VCH, 2008.
2 R. P. Swatloski, R. D. Rogers and J. D. Holbrey, Dissolution and processing of cellulose using ionic liquids, *Int. Pat.*, WO 03/029329, 2003.
3 M. J. Earle, J. Esperanca, M. A. Gilea, J. N. C. Lopes, L. P. N. Rebelo, J. W. Magee, K. R. Seddon and J. A. Widegren, *Nature*, 2006, **439**, 831.
4 P. Wasserscheid, *Nature*, 2006, **439**, 797.
5 F. Endres and S. Z. El Abedin, *Phys. Chem. Chem. Phys.*, 2006, **8**, 2101.
6 T. Welton, *Coord. Chem. Rev.*, 2004, **248**, 2459.
7 J. L. Anderson, D. W. Armstrong and G. T. Wei, *Anal. Chem.*, 2006, **78**, 2892.
8 C. Jork, C. Kristen, D. Pieraccini, A. Stark, C. Chiappe, Y. A. Beste and W. Arlt, *J. Chem. Thermodyn.*, 2005, **37**, 537.
9 M. Maase and K. Massonne, in *Ionic Liquids IIIB: Fundamentals, Progress, Challenges and Opportunities: Transformations and Processes*, ed. R. D. Rogers and K. R. Seddon, ACS Symp. Ser., 2005, vol. 902, pp. 126–132.
10 A. E. Visser, R. P. Swatloski, W. M. Reichert, R. Mayton, S. Sheff, A. Wierzbicki, J. H. Davis and R. D. Rogers, *Chem. Commun.*, 2001, 135.
11 T. J. Gannon, G. Law, P. R. Watson, A. J. Carmichael and K. R. Seddon, *Langmuir*, 1999, **15**, 8429.
12 G. Law, P. R. Watson, A. J. Carmichael, K. R. Seddon and B. Seddon, *Phys. Chem. Chem. Phys.*, 2001, **3**, 2879.
13 C. Hardacre, *Annu. Rev. Mater. Res.*, 2005, **35**, 29.
14 N. V. Plechkova and K. R. Seddon, *Chem. Soc. Rev.*, 2008, **37**, 123.
15 C. Aliaga, C. S. Santos and S. Baldelli, *Phys. Chem. Chem. Phys.*, 2007, **9**, 3683.
16 M. Mezger, H. Schroder, H. Reichert, S. Schramm, J. S. Okasinski, S. Schoder, V. Honkimaki, M. Deutsch, B. M. Ocko, J. Ralston, M. Rohwerder, M. Stratmann and H. Dosch, *Science*, 2008, **322**, 424.
17 P. J. Carvalho, M. G. Freire, I. M. Marrucho, A. J. Queimada and J. A. P. Coutinho, *J. Chem. Eng. Data*, 2008, **53**, 1346.

18 S. Baldelli, *Acc. Chem. Res.*, 2008, **41**, 421.
19 A. Riisager, P. Wasserscheid, R. van Hal and R. Fehrmann, *J. Catal.*, 2003, **219**, 452.
20 A. Riisager, R. Fehrmann, M. Haumann and P. Wasserscheid, *Top. Catal.*, 2006, **40**, 91.
21 M. Haumann and A. Riisager, *Chem. Rev.*, 2008, **108**, 1474.
22 D. H. Zaitsau, G. J. Kabo, A. A. Strechan, Y. U. Paulechka, A. Tschersich, S. P. Verevkin and A. Heintz, *J. Phys. Chem. A*, 2006, **110**, 7303.
23 J. P. Armstrong, C. Hurst, R. G. Jones, P. Licence, K. R. J. Lovelock, C. J. Satterley and I. J. Villar-Garcia, *Phys. Chem. Chem. Phys.*, 2007, **9**, 982.
24 J. P. Leal, J. Esperanca, M. E. M. da Piedade, J. N. C. Lopes, L. P. N. Rebelo and K. R. Seddon, *J. Phys. Chem. A*, 2007, **111**, 6176.
25 S. Krischok, M. Eremtchenko, M. Himmerlich, P. Lorenz, J. Uhlig, A. Neumann, R. Ottking, W. J. D. Beenken, O. Hofft, S. Bahr, V. Kempter and J. A. Schaefer, *J. Phys. Chem. B*, 2007, **111**, 4801.
26 S. Caporali, U. Bardi and A. Lavacchi, *J. Electron Spectrosc. Relat. Phenom.*, 2006, **151**, 4.
27 K. Nakajima, A. Ohno, M. Suzuki and K. Kimura, *Nucl. Instrum. Methods Phys. Res. Sect. B-Beam Interact. Mater. Atoms*, 2009, **267**, 605.
28 S. Rivera-Rubero and S. Baldelli, *J. Phys. Chem. B*, 2006, **110**, 4756.
29 C. S. Santos and S. Baldelli, *J. Phys. Chem. B*, 2007, **111**, 4715.
30 C. S. Santos, S. Rivera-Rubero, S. Dibrov and S. Baldelli, *J. Phys. Chem. C*, 2007, **111**, 7682.
31 C. S. Santos and S. Baldelli, *J. Phys. Chem. B*, 2009, **113**, 923.
32 T. Iimori, T. Iwahashi, K. Kanai, K. Seki, J. H. Sung, D. Kim, H. O. Hamaguchi and Y. Ouchi, *J. Phys. Chem. B*, 2007, **111**, 4860.
33 Y. Jeon, J. Sung, W. Bu, D. Vaknin, Y. Ouchi and D. Kim, *J. Phys. Chem. C*, 2008, **112**, 19649.
34 J. Bowers, M. C. Vergara-Gutierrez and J. R. P. Webster, *Langmuir*, 2004, **20**, 309.
35 E. Solutskin, B. M. Ocko, L. Taman, I. Kuzmenko, T. Gog and M. Deutsch, *J. Am. Chem. Soc.*, 2005, **127**, 7796.
36 A. P. Froba, H. Kremer and A. Leipertz, *J. Phys. Chem. B*, 2008, **112**, 12420.
37 M. G. Freire, P. J. Carvalho, A. M. Fernandes, I. M. Marrucho, A. J. Queirnada and J. A. P. Coutinho, *J. Colloid Interface Sci.*, 2007, **314**, 621.
38 V. Halka, R. Tsekov and W. Freyland, *Phys. Chem. Chem. Phys.*, 2005, **7**, 2038.
39 Y. F. Yano and H. Yamada, *Anal. Sci.*, 2008, **24**, 1269.
40 W. Jiang, Y. T. Wang, T. Y. Yan and G. A. Voth, *J. Phys. Chem. C*, 2008, **112**, 1132.
41 R. M. Lynden-Bell and M. Del Popolo, *Phys. Chem. Chem. Phys.*, 2006, **8**, 949.
42 T. M. Chang and L. X. Dang, *J. Phys. Chem. A*, 2009, **113**, 2127.
43 N. Sieffert and G. Wipff, *J. Phys. Chem. C*, 2008, **112**, 6450.
44 M. P. Seah and W. A. Dench, *Surf. Interface Anal.*, 1979, **1**, 2.
45 I. S. Tilinin, A. Jablonski and W. S. M. Werner, *Prog. Surf. Sci.*, 1996, **52**, 193.
46 E. F. Smith, I. J. Villar Garcia, D. Briggs and P. Licence, *Chem. Commun.*, 2005, 5633.
47 E. F. Smith, F. J. M. Rutten, I. J. Villar-Garcia, D. Briggs and P. Licence, *Langmuir*, 2006, **22**, 9386.
48 S. Krischok, R. Ottking, W. J. D. Beenken, M. Himmerlich, P. Lorenz, O. Hofft, S. Bahr, V. Kempter and J. A. Schaefer, *Z. Phys. Chem.*, 2006, **220**, 1407.
49 O. Hofft, S. Bahr, M. Himmerlich, S. Krischok, J. A. Schaefer and V. Kempter, *Langmuir*, 2006, **22**, 7120.
50 J. M. Gottfried, F. Maier, J. Rossa, D. Gerhard, P. S. Schulz, P. Wasserscheid and H. P. Steinruck, *Z. Phys. Chem.*, 2006, **220**, 1439.
51 F. Maier, J. M. Gottfried, J. Rossa, D. Gerhard, P. S. Schulz, W. Schwieger, P. Wasserscheid and H. P. Steinruck, *Angew. Chem., Int. Ed.*, 2006, **45**, 7778.
52 D. S. Silvester, T. L. Broder, L. Aldous, C. Hardacre, A. Crossley and R. G. Compton, *Analyst*, 2007, **132**, 196.
53 V. Lockett, R. Sedev, C. Bassell and J. Ralston, *Phys. Chem. Chem. Phys.*, 2008, **10**, 1330.
54 C. Kolbeck, M. Killian, F. Maier, N. Paape, P. Wasserscheid and H. P. Steinruck, *Langmuir*, 2008, **24**, 9500.
55 N. Paape, W. Wei, A. Bosmann, C. Kolbeck, F. Maier, H. P. Steinruck, P. Wasserscheid and P. S. Schulz, *Chem. Commun.*, 2008, 3867.
56 T. Cremer, M. Killian, J. M. Gottfried, N. Paape, P. Wasserscheid, F. Maier and H. P. Steinruck, *ChemPhysChem*, 2008, **9**, 2185.
57 K. R. J. Lovelock, C. Kolbeck, T. Cremer, N. Paape, P. S. Schulz, P. Wasserscheid, F. Maier and H. P. Steinruck, *J. Phys. Chem. B*, 2009, **113**, 2854.
58 C. Kolbeck, T. Cremer, K. R. J. Lovelock, N. Paape, P. S. Schulz, P. Wasserscheid, F. Maier and H. P. Steinruck, *J. Phys. Chem. B*, 2009, **113**, 8682.
59 A. Heintz, *J. Chem. Thermodyn.*, 2005, **37**, 525.
60 R. F. Roberts, D. L. Allara, C. A. Pryde, D. N. E. Buchanan and N. D. Hobbins, *Surf. Interface Anal.*, 1980, **2**, 5.
61 Z. F. Fei, W. H. Ang, D. B. Zhao, R. Scopelliti, E. E. Zvereva, S. A. Katsyuba and P. J. Dyson, *J. Phys. Chem. B*, 2007, **111**, 10095.
62 G. D. Smith, O. Borodin, L. Y. Li, H. Kim, Q. Liu, J. E. Bara, D. L. Gin and R. Nobel, *Phys. Chem. Chem. Phys.*, 2008, **10**, 6301.
63 A. S. Duwez, *J. Electron Spectrosc. Relat. Phenom.*, 2004, **134**, 97.
64 T. Cremer, C. Kolbeck, K. R. J. Lovelock, N. Paape, P. S. Schulz, P. Wasserscheid, F. Maier and H. P. Steinruck, 2009, unpublished work.
65 J. M. Slattery, C. Daguenet, P. J. Dyson, T. J. S. Schubert and I. Krossing, *Angew. Chem., Int. Ed.*, 2007, **46**, 5384.
66 Y. J. Nikas, S. Puvvada and D. Blankschtein, *Langmuir*, 1992, **8**, 2680.
67 K. R. J. Lovelock, C. Kolbeck, T. Cremer, N. Paape, J. Lehmann, A. P. Froba, P. Wasserscheid, F. Maier and H. P. Steinruck, 2009, unpublished work.